SEDs vs. Emission-Line Correlations in Low Redshift Quasars

Joanna Kuraszkiewicz[1], Belinda J. Wilkes, Paul J. Green, Smita Mathur, & Jonathan C. McDowell, Bożena Czerny[2]

SAO, Cambridge, MA, USA

Abstract. We investigate the relations between the observed emission line strengths, widths and continuum properties of a sample of low redshift quasars for which contemporaneous IR-soft-X-ray spectral energy distributions (SEDs) are available. This includes investigating correlations between optical/UV lines with both the luminosity and the shape of the quasars' continua, as well as correlations between the various lines. Our data do not favor a model in which changes in continuum shape (due to e.g. ionization parameter decreasing with luminosity) cause the Baldwin effect. The data can instead be explained by an accretion disk (AD) model in which limb darkening and the projected surface area of an optically thick, geometrically thin disk combine to cause a viewing-angle dependent apparent optical/UV (OUV) luminosity and a more isotropic X-ray luminosity. The scatter in our correlations is larger than that expected from this AD model, suggesting the presence of dust which reddens both the continuum and the broad emission lines. We also look in greater detail at the line properties of NLS1 galaxies which do not follow the Baldwin effect for the remainder of the sample and discuss reasons for the discrepancy.

1. Introduction

The strong, broad emission lines which characterize quasar spectra are generally believed to be generated in a large number of small gas clouds photoionized by the central continuum source of a quasar. To date photoionization models have been reasonably successful in predicting the average emission line properties of a quasar using an average continuum shape. However it has become clear that, while the emission line properties are largely similar from quasar to quasar, the observed spectral energy distributions (SEDs) are not (Elvis et al. 1994). If photoionization models are generally applicable, we would expect systematic relations between the observed lines and continuum in different objects (Krolik & Kallman 1988) and, at first glance at least, the dichotomy between continuum and the line behavior looks surprising. We will show that this behavior can be

---

[1] also N. Copernicus Astronomical Center, Warsaw, Poland

[2] N. Copernicus Astronomical Center, Warsaw, Poland

explained by an accretion disk model, surrounded by a dusty torus, with the addition of small amounts of dust reddening both the lines and the continuum.

2. Sample

We have obtained a small sample of uniform, high quality continuum and emission line data. The sample consists of 41 low redshift ($z < 1$) quasars, among which 18 are radio-loud, selected to have high-quality X-ray data in the Einstein archives. We have obtained far-infrared (IR) through soft X-ray (100 μm – 3.5 keV) continuum data and low-resolution (5-20Å) optical (our observations) and ultraviolet spectra (IUE archives). We have measured all the line and continuum parameters ourselves to minimize the scatter generally introduced by combining datasets from different techniques and different analysis. The range in shapes of the IR–ultraviolet continuum is large even in this small, low-redshift sample, allowing investigation of whether the range in continuum shapes produces any corresponding range in the emission line properties. The X-ray selection results in a bias towards low α_{ox} quasars.

3. Analysis and Results

We investigate the relations between various emission line parameters (fluxes, equivalent widths (EW) and full-width at half maximum intensity (FWHM) of all the prominent optical and UV emission lines) and continuum parameters (L_{opt}, L_X, decade and octave luminosities, broad-band luminosities: L_{UVOIR}, L_{BOL}, Lycon, L_{Ion} and spectral slopes: α_{ox}, α_x, α_{OUV}). We use the ASURV statistical package (Isobe, Feigelson, & Nelson 1986) which includes allowance for the presence of upper limits in the sample. Specifically we applied the following tests to each pair of parameters: the Generalized Kendall Rank and the Spearman Rank test, which is insensitive to outlying points. We considered a correlation real only if the probability of it occurring by chance was <2% in *both* of these tests. We also look for primary correlations among the line/continuum relations ie. test which correlation is strongest, while other variables are held constant.

We find anticorrelations between the equivalent-width (EW) and various OUV luminosities for the Lyα and Hβ lines (Fig.1a,b) and a marginal anticorrelation for CIII]. Here we use the expression "Baldwin effect" (BEff) in a general sense to refer to an anticorrelation of line EW with any OUV luminosity. The exclusion of seven narrow line, low luminosity AGN reveals similar BEff relation for both CIII] and CIV lines (Fig. 1c). This suggests that NLS1s have systematically low carbon line EW for their luminosity. We will return to this problem in Section 5.

A significant anticorrelation with α_{ox} is seen for the EW of CIV line (Fig. 1d), and a marginal anticorrelation for Hβ and OVI. We do not find any correlations between lines and the X-ray luminosity or X-ray slope. The FeII optical multiplet also does not show a simple relationship with luminosity or continuum slope, however there is a tendency for objects with flat X-ray spectra and/or strong X-ray luminosities to have weak FeII.

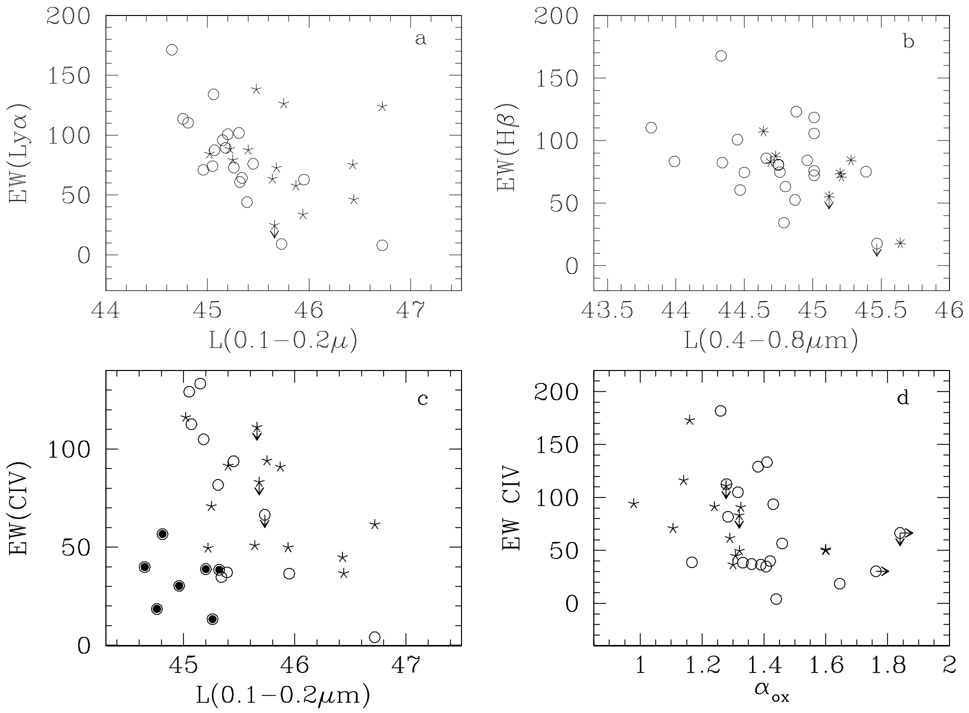

Figure 1. a,b,c - Correlations between line equivalent widths and luminosity. Radio-loud quasars are indicated by stars and radio-quiet by circles; upper limits by arrows. In Fig. 1c filled circles denote NL S1 objects which destroy the CIV Baldwin effect. d - Correlation between CIV equivalent width and α_{ox}.

4. The Baldwin Effect

The inverse correlation between the emission line equivalent widths and the UV luminosity is commonly known as the Baldwin effect (Baldwin 1977). It indicates that the line flux is increasing more slowly than the local continuum (i.e. is constant) as the quasar luminosity increases. It has been shown that the Baldwin effect in CIV and Lyα lines covers 7 orders of magnitude in quasar luminosity (Kinney et al. 1990). In comparison our sample covers ~ 2 orders of magnitude and shows a steeper slope in the $EW(L)$ relation. There have been a number of explanations for the BEff suggested:

Zheng & Malkan (1993) - explain it as due to the shift of the big blue bump towards lower energies with increasing luminosity. Hence the higher luminosity quasars have a lower fraction of higher energy ionizing photons. This causes the equivalent widths of high ionization emission lines sensitive to the X-ray continuum (CIV and HeII) to decrease at high luminosities relative to lower-ionization emission lines (Lyα, CIII], and the Balmer lines). The scenario thus predicts a stronger and more easily detectable Baldwin effect for higher-ionization lines. Our data do not favor this model as we see the Baldwin effect equally for both high and low-ionization lines.

Mushotzky & Ferland (1984) - explain the Baldwin effect as due to a systematic decrease in ionization parameter, U, as the luminosity increases. As the ionization parameter depends on the number of ionizing photons, U depends on the continuum shape.

The model predicts the Baldwin effect for the CIV line only, as the CIV line luminosity increases rapidly with increasing U (decreasing UV luminosity and α_{ox} - see Fig.1 in Mushotzky & Frland 1984). The Lyα, CIII], Hα, and Hβ do not show any Baldwin effect in this scenario. Additionally equivalent widths of Lyα, CIII], CIV should be, according to the model, relatively independent of both α_{ox} and α_x as the lines do not originate in the X-ray heated zones deep in the emission-line clouds. The model is not consistent with our data.

The Accretion Disk (AD) Model - Netzer (1985,1987), Netzer et al. (1992) If the optically thick accretion disk, in the center of an AGN, is geometrically thin, then limb darkening and change in projected surface area will result in a range of apparent OUV luminosities if the disk is viewed from different angles. The UV emission is strongest when the disk is viewed face-on, while the X-ray emission is more isotropic. The BELR radiates isotropically as the clouds are at distances greater than the size of the UV-emitting part of the disk. The differing viewing angle dependence of the lines and the continuum results in an anticorrelation of line equivalent widths with OUV luminosity and α_{ox}. For the more isotropic X-ray emission, such correlations are not expected. The predictions of this model are consistent with our data.

The AD model predicts both the slope of the line vs. driving continuum (ie. heating/ionizing continuum defined after Krolik & Kallman 1988) correlations and scatter around the mean. Both are dependent on the range of disk inclination angles seen by the observer and the luminosity range of the observed sample. For a larger range in both disk inclinations and/or observed range of luminosities the slopes are flatter and the scatter larger. Most of the lines vs. driving continuum correlations (except for CIII] and CIV which are also collisionally excited) have slopes as predicted by the model, with the assumption that a dusty torus with a standard opening angle of 60^0 obscures the AD (and prevents the observer seeing the AGN at larger viewing angles).

The scatter around the mean slope in our sample is larger than that expected from the model. We interpret this as due to random obscuration of lines and continuum by dust lying outside the BLR.

4.1. The role of dust

Several properties of our sample suggest the presence of dust: first we see larger Balmer decrements than the canonical "case B" value, second the primary correlations between lines and continua are *not* with their driving continuum.

To check how dust can change the primary correlations and how much scatter it can produce, we have constructed a hypothetical sample of objects, having a range in bolometric luminosity matching our real sample, and reddened by a random amount of dust, the maximum reddening was based on the range of big blue bump (BBB) strengths in the real sample. Before being reddened each hypothetical object was assumed to have a SED matching the quasar with the largest BBB in the real sample (PG 1426+015). We have chosen two extinction curves: the standard Galactic extinction curve (Seaton 1979) and the Small Magellanic Cloud (SMC) extinction curve (Prévot et al. 1984), which corresponds well to the extinction by dust dominated by small amorphous carbon grains (Czerny et al. 1995). Two lines widely separated in wavelength, Lyα and Hβ, were studied. We found that the hypothetical sample randomly reddened by dust lying outside the BLR, with maximum extinction $E(B-V) = 0.2$, and following the SMC extinction curve, has the same primary correlations for Lyα and Hβ lines as the real sample. The scatter in the line vs. driving continuum correlations is comparable to the additional scatter required in comparing our results with the accretion disk model.

We conclude that the Netzer AD disk model surrounded by an optically thick dusty torus with a 60^0 opening angle, and addition of small amounts of dust outside the BLR (reddening both the lines and continuum) explains well our observed line-continuum correlations.

4.2. How does our sample fit into the global Baldwin effect?

The BEff has been seen to cover many orders of magnitude in L_{UV}. A comparison with the sample of Kinney et al. (1990), which shows a BEff for Lyα and CIV lines over 7 orders of magnitude in luminosity, reveals that our sample, which covers only a factor of 100 in L_{UV}, has a steeper slope of the BEff. This is in agreement with the AD model predictions, as samples with smaller luminosity range should show in the EW vs L_{UV} diagram mostly the dependence from the disk inclination (hence having steeper slopes - see Netzer et al. 1992) which in larger luminosity range samples is superposed with other processes and adds only scatter to the general BEff. So one possible way of reducing the BEff scatter, and hence opening the possibility of using the BEff as a standard candle would be to select sources with a small range of orientation.

As has also been shown in Fig.1c NLS1s are sampling a different region of the BEff, suggesting that selection of objects with the similar FWHM could reduce the scatter in the BEff.

5. NLS1

Having found that NLS1 galaxies follow a different BEff relations for CIV (Fig.1c) we decided to look more carefully at the UV spectra of this class of objects. We have compiled from the literature a list of all currently known NLS1s and looked for their UV spectra in the HST and IUE archives. We ended up with a sample of 11 objects, for which emission line properties were compared with typical broad-line AGN (Seyfert 1 and quasars). The CIV equivalent widths of NLS1s were found to be significantly smaller than the EW of all other broad-line AGN. Also the CIII]/Lyα, CIV/Lyα ratios, when compared to these AGN, appeared smaller (Fig.2). As the carbon lines are collisionally excited, they are sensitive to the cloud densities at which they form. They are also a sensitive function of the ionization parameter U. Therefore to find what parameters can cause such

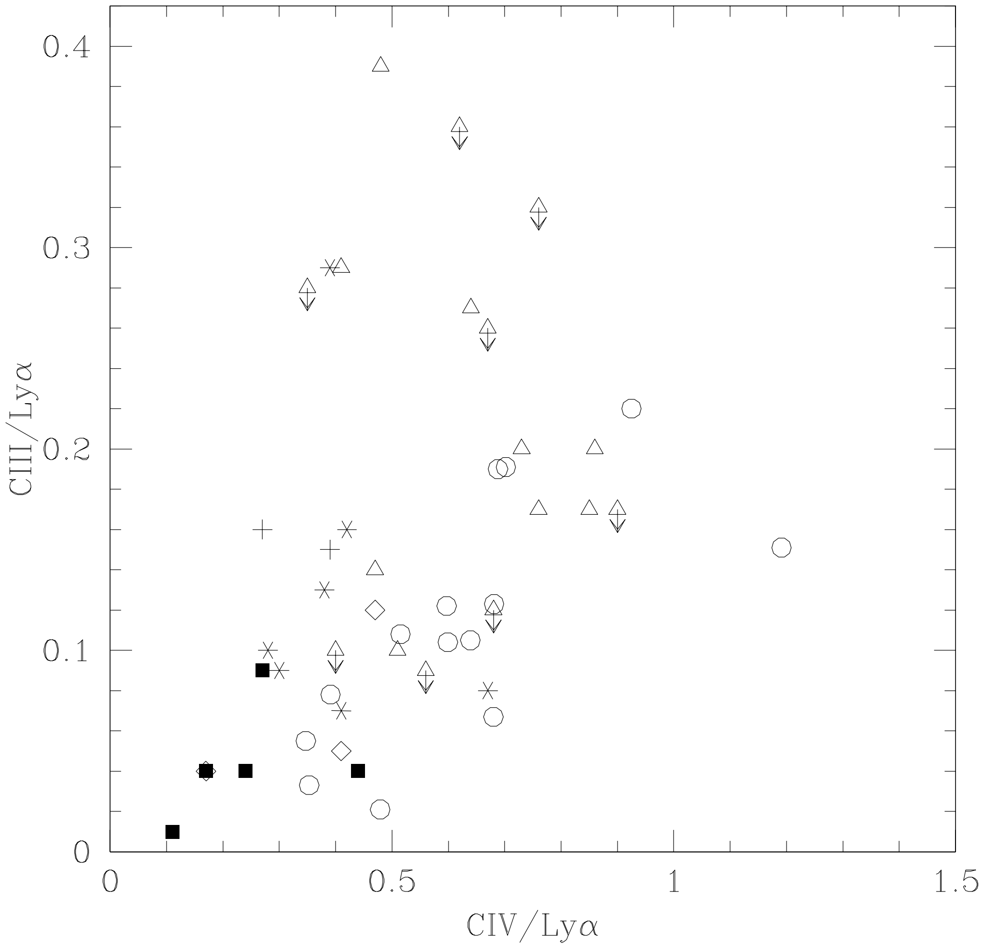

Figure 2. Comparison of CIII/Lyα and CIV/Lyα ratios for NLS1 objects (filled squares) and Seyfert 1 galaxies from Wu et al. (1983, circles) and QSOs from Laor et al. (1995, stars), Christiani & Vio (1990, crosses), Wilkes et al. (1998, triangles) and narrow line quasars from Baldwin et al. (1988, diamonds). (For CIII we used the sum of CIII+SiIII+AlIII to allow comparison with other samples were broad lines unabled the authors to separate these components.)

small ratios and small EW, we calculated the CIII]/Lyα and CIV/Lyα ratios for different densities and U using the ionization code *Cloudy* (Ferland 1991) and the input ionizing continuum of one of our NLS1s (PG 1211+143). The results are presented in Fig.3, where filled circles represent values of line ratios for $logU = -3$ (where $U = \frac{\int_{1Ryd}^{\infty} \frac{L_\nu}{h\nu}}{4\pi r^2 c n_H}$), open squares $logU = -2$, and triangles $logU = -1$; horizontal lines show the observed values. It is clear from the figure that in order to produce such small carbon to Lyα ratios as seen in NLS1s, a smaller ionization parameter ($logU = -3$) and densities larger (by factor 10-100) than standard ($logU = -2, \rho = 10^{9.5} cm^{-3}$) are needed. We have also found that the SiIII]λ1892/CIII]λ1909 and SiIV+OIV]λ1400/CIVλ1549 ratios are larger and that AlIIIλ1857 is stronger than in other broad-line AGN. This is also consistent with higher densities of the emitting line region (see Rees, Netzer, Ferland 1989, Korista et al. 1996). SiIII] is thermalized at a higher critical density than CIII], so higher SiIII]/CIII] ratios indicate higher densities. Also at densities higher than critical CIV and Lyα are no longer efficient coolants and other ions such as AlIIIλ1857 take over the cooling resulting in stronger lines.

5.1. Why do NLS1 BLR cloud have higher densities?

The broad line region (BLR) gas which is Compton heated will form two phases: a cool phase with $T \sim 10^4$ (the BLR clouds) and a hot phase with $T \sim 10^8$ (the intercloud medium) (see eg. Krolik & Kallman 1988, Czerny & Dumont 1998, Wandel & Liang 1991). Precise values of these temperatures depend on the shape of the continuum.

It is known (eg. Puchnarewicz et al. 1995, Boller, Brandt & Fink 1996) that the big blue bumps (BBBs) of NLS1s are shifted towards higher energies compared to other AGN. It has been suggested that this is due to higher ratios of their luminosity to the Eddington luminosity ie. systematically lower masses (factor of 100) at a given luminosity range than other AGN (Pounds, Done & Osborne 1995, Wandel 1997). Krolik & Kallman (1988) calculated that for a NLS1 spectrum the Compton temperature of the hot (intercloud) medium is smaller by a factor of 4, when compared with a "normal" AGN spectrum, while the temperature of the cold phase is 10 times larger. The density of the BLR clouds should also change due to the change in the intrinsic spectrum and we will now estimate exactly by how much. We use the ionization parameter of Krolik, McKee & Tarter (1981):

$$\Xi = \frac{2.3 F_{ion}}{cp} = \frac{2.3 F_{ion}}{\frac{ck\rho T_c}{\mu H}} \tag{1}$$

where F_{ion} is the flux above 1 Ryd determined by the ionizing luminosity of the central source, L_{ion}, and the current radius r (where effects of geometry have been neglected):

$$F_{ion} = L_{ion}/4\pi r^2. \tag{2}$$

The two phases coexist at the value of the ionization parameter Ξ_h which scales with the hot phase temperature T_h in the following way (Begelman 1983):

$$\Xi_h = 0.65 \left(\frac{T_h}{10^8}\right)^{-3/2} \tag{3}$$

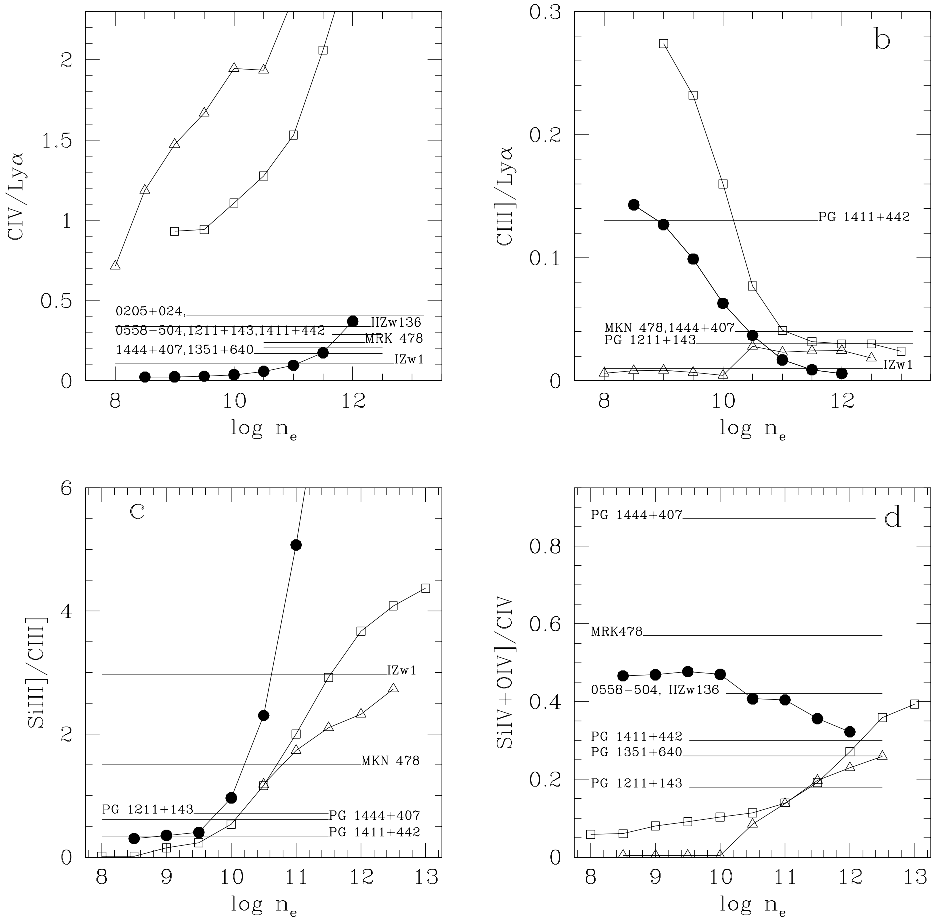

Figure 3. Calculated line ratios a) CIV/Lyα, b) CIII]/Lyα, c) SiIII]/CIII], d) SiIV+OIV]/CIV for different ionization parameters. Triangles denote $U = -1$, squares $U = -2$ and filled circles $U = -3$. Horizontal lines show the values of the observed line ratios

The BLR is most probably radially extended. However, for the purposes of this estimation we determine a representative radius. If the cloud number density profile is flatter than r^{-2}, then most of the emission would come from the outer radii of the BLR. As in the case of the Inverse Compton heated coronae discussed by Begelman et al. (1983), a nearly hydrostatic corona will exist up to a radius where the temperature of the hot medium is equal to the "escape" temperature (ie. the virial temperature). For larger radii the temperature of the corona is larger than the virial temperature, the corona becomes unstable and is blown away in a form of a wind. We therefore identify the outer edge of the BLR r_{BLR} with the radius at which the hot medium temperature is equal to the virial temperature:

$$kT_h = \frac{GMm_H}{r_{BLR}}. \tag{4}$$

Combining equations (1)-(4) we estimate the cloud density:

$$\rho_{cold} \sim \frac{L}{M^2} \times \frac{T_h^{7/2}}{T_{cold}} \tag{5}$$

Remembering that for the same luminosity range masses of the central black hole in NLS1s are a factor of 100, T_h a factor 4 smaller as compared to other AGN, and T_{cold} is a factor 10 larger, this implies that the densities of the BLR should be an order of magnitude higher in NLS1 than in typical AGN. This is consistent with the results previously obtained from line ratios.

Acknowledgments. BJW, JCM, PJG acknowledge support provided by NASA through Contract NAS8-39073 (ASC), JK a Smithsonian pred-doc. fellowship at Harvard-Smithsonian Center for Astrophysics and KBN grant 2P03D00410. SM acknowledges support by NASA grant NAG5-3249 (LTSA) and PJG grant HF-1032.01-92A awarded by the Space Telescope Science Institute, which is operated by the Association of Universities for Research in Astronomy, Inc., under NASA contract NAS5-26555.

References

Baldwin, J.A., 1977, ApJ, 214, 679

Baldwin, J.A., McMahon, R., Hazard, C., Williams, R.E., 1988, ApJ, 327, 103

Begelman M. C., McKee, C. F., Shields, G. A., 1983, ApJ, 271, 70

Boller, Th., Brandt, W.N., Fink, H., 1996, AA 305, 53

Christiani, S. & Vio, R., 1990, AA, 227, 385

Czerny, B., Loska, Z., Szczerba, R., Cukierska, J., Madejski, G. 1995, Acta Astron. 45, 623.

Czerny, B., Dumont, A.-M., 1998, astro-ph/9808014, to appear in AA

Elvis, M., Wilkes, B.J., McDowell, J.C., Green, R.F., Bechtold, J., Willner, S.P., Oey, M.S., Polomski, E., Cutri, R., 1994, ApJS, 95, 1

Ferland, G.F., 1991, "HAZY", OSU Astronomy Department Internal Report

Isobe, T., Feigelson, E.D., & Nelson P.I. 1986, ApJ, 306, 490.

Kinney, A.L., Rivolo, A.R., & Koratkar, A.P. 1990, ApJ, 357, 338.

Korista, K., Baldwin, J., Ferland, G., Vermer D., 1996, ApJS, 108, 401

Krolik, J.H., McKee, C.F., Tarter, C.B., 1981, ApJ, 249, 422

Krolik, J.H., & Kallman, T.R. 1988, ApJ, 324, 714.

Laor, A., Bahcall, J.N., Jannuzi, B.T., Schneider, D.P., Green, R.F., 1995, ApJS, 99, 1

Mushotzky, R., & Ferland, G.J. 1984, ApJ, 278, 558.

Netzer, H. 1985, MNRAS, 216, 63.

Netzer, H. 1987, MNRAS, 225, 55 .

Netzer, H., Laor, A., & Gondhalekar, P.M. 1992, MNRAS, 254, 15.

Pounds, K.A., Done, C., & Osborne J., 1995, MNRAS, 277, L5

Prévot, M.L., Lequeux, J., Maurice, E., Prévot, E., & Rocca-Volmerange, B. 1984, A&A, 132, 389.

Puchnarewicz, E.M., Mason, K.O., Siemiginowska, A., Pounds, K.A., 1995, MNRAS, 276, 20

Rees, M.J., Netzer, H., Ferland G.J, 1989, ApJ, 347, 640

Seaton, M.J. 1979, MNRAS, 187, 73P.

Wandel, A., 1997, ApJ, 490, L131

Wandel, A., & Liang, E.P., 1991, ApJ, 380, 84

Wilkes B.J., Kuraszkiewicz, J. Green, P.J., Mathur, S., McDowell, J.C., 1998, submitted to ApJ

Wu C.-C., Boggess, A., Gull, T.R., 1983, ApJ, 266, 28

Zheng, W., & Malkan, M.A. 1993, ApJ, 415, 517.